THE INTERNATIONAL JOURNAL OF SCIENCE & TECHNOLEDGE

Investigation on Spectral, Optical, Energy Level Designation of 6-(2-Phenylhydrazono) Tetrahydro-2-Thioxopyrimidin-4(1H)-one using Experimental and Theoretical Methods

Natarajan Kalaiarasi
Research Scholar, Post Graduate and Research Department of Chemistry,
Government Arts College, C. Mutlur, Chidambaram, Tamil Nadu, India
Dr. Subramaniyan Manivarman
Assistant Professor, Post Graduate and Research Department of Chemistry,
Government Arts College, C-Mutlur, Chidambaram, Tamil Nadu, India

Abstract:
6 - (2 - phenylhydrazono) tetrahydro – 2-thioxo-pyrimidin – 4(1H)-one was synthesized and characterized using FT-IR, FT-Raman, NMR spectral techniques. The FT-IR and FT-Raman spectra of 6-(2–phenylhydrazono)–tetrahydro–2–thioxo-pyrimidin-4(1H)-one have been recorded in order to study the normal modes of vibrations. The theoretical wave number predictions were calculated by the density functional theory using the B3LYP function with 6-31G (d, p) basis set. Vibrational assignments were assigned with the help of potential energy distribution analysis. The first order hyperpolarizability (β_o) calculation was performed to investigate the optical behaviour of the compound. The energy levels designated with respect to transition of electron from lower (σ) to higher level (π). The UV absorption at 238nm is designated as R-bands due to π - π^*. Stability of the molecule arising from hyper-conjugative interactions between donor (i) and acceptor (j) orbitals of the molecule. Global reactivity descriptors and thermodynamic properties of PHTTO have also calculated based on DFT calculations.

Keywords: *Thioxo-pyrimidine, NBO, HOMO – LUMO, NLO, PED.*

1. Introduction

2-thiobarbituric acid scaffold consists of a pyrimidine cyclic structure and have a large number of biological application. Thiobarbituric acid and their derivatives are pharmacologically important such as intravenous anesthetics [i], anticonvulsants [ii], immunotropic [iii], anti-inflammatory[iv], antibacterial activity [v], sedatives [vi], herbicides [vii], antiviral agents, antihyperthyroid [viii], membrane protector [*ix*], radio protector [*x*],thermal stabilizers [xi] and used to measure the auto-oxidation of brain homogenates for various animals [xii], treat non-alcoholic fatty liver disease [xiii], and determine formaldehyde and acetaldehyde in the food [xiv]as well as they form a type of bioactive complex with triphenyltin. A large number of reports are available on the reactions of thiobarbituric acid with carbonyl compounds-aldehydes, ketones and esters [xv-xvi]. Reaction of thiobarbituric with phenyl hydrazine results in formation of hydrazone linkaged product. The substituent phenyl hydrazine has haemolytic and antipyretic action, as well as used in manufacturing dyes, reagent for sugars, stabilizer for explosives [xvii].

Hydrazones are a special class of organic compounds in the Schiff base family [xviii]. The hydrazone linkage are represented by C=N-NH. The C and N are the active centers of hydrazone mainly responsible for physical and chemical properties due to the reactivity towards electrophiles and nucleophiles. The usefulness has leaded the hydrazones to emerge as good chelating agents that can form a variety of complexes with different transition metals [xviii]. Hydrazones and their derivatives are known to exhibit a wide range of interesting biological activities like antioxidant, analgesic, anticancer, antiprotozoal, antiparasitic, antiplatelet, cardio-protective, anthelmintic, antidiabetic, antitubercular, trypanocidal, anti-HIV, potent anti-inflammatory [xix-xx].

In the present report, the structural conformation, vibrational Assignments other thermodynamic parameters of title molecules were investigated using DFT calculations. Organic materials play a major role in non-linear optics due to their great optical behaviour hence we investigated the first hyperpolarizability coefficient energy gap through DFT and UV-visible spectrum. Intra molecular charge transfer in the molecule is analyzed by NBO analysis.

2. Experimental Section

2.1. Synthesis of Thiobarbituric acid

About 6g (0.25mol) of sodium metal is dissolved in 200ml of ethanol. To this solution 15g (0.25mol) of thiourea and 40ml of diethyl malonate is added. The reaction mixture is refluxed for 6hrs. in an oil bath and then vacuum distillated to make ethanol recovery. The clear solution thus obtained is filtered, cooled in ice bath overnight and the resulting solution is acidified with HCl. The crude product obtained is collected, washed with 50ml water and dried in oven at 105-110°C for nearly 4 hrs. The obtained compound purified by recrystallization with ethanol. (Melting point- 243°C, yield-80%).

2.2. Synthesis of 6-(2-phenylhydrazono)-tetrahydro-2-thioxopyrimidin-4(1H)-one

Equimolar mixture of thiobarbituric acid 2.44g (0.1mol), phenyl hydrazine 2.08g (0.1mol) are dissolved in ethanol, the content is condensed on oil bath for 4 hours, then the reaction mixture is stand overnight and the precipitate obtained is filtered washed with ethanol and dried to obtain the pale yellow powder product, the product thus obtained is recrystallized (Melting point - 180^{0}C, yield – 67%).

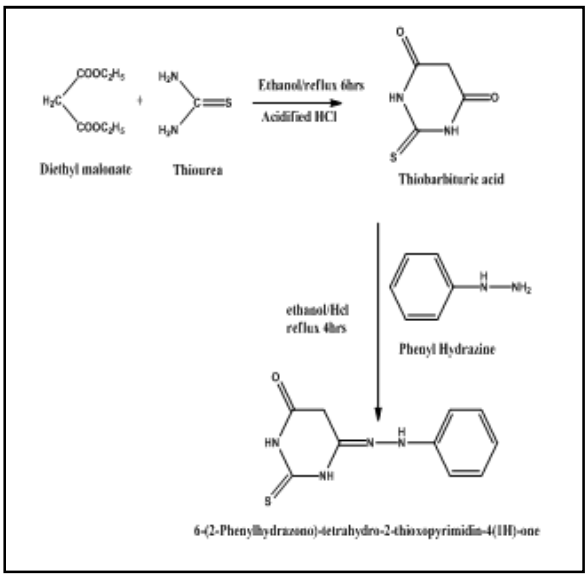

Figure 1

2.3. Mechanism of the Reaction

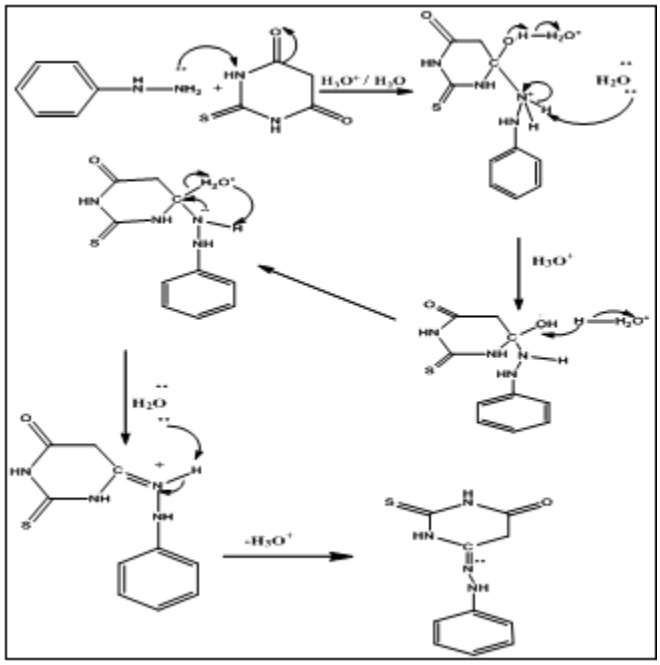

Figure 2

2.4. Materials and Methods

All the solvents used were of spectral grade. The melting points of the compound were measured in open capillaries and are uncorrected. IR spectra were recorded on an AVATAR-330 FT-IR spectrometer with spectral range of 4000-400 cm^{-1}. FT-Raman spectrum was recorded on BRUKER: RFS 27 with spectral range of 3500-50 cm^{-1}. ^{1}H NMR spectrum was recorded at 400 MHz and ^{13}C NMR spectrum at 100MHz on a BRUKER model using DMSO-*d6* as solvent. Tetramethylsilane (TMS) was used as internal reference for all NMR spectra, with chemical shifts reported in δ units (parts per million) relative to the standard.

2.5. Quantum Chemical Calculations

Calculations of the title compound were carried out with Gaussian 03 software program using the B3LYP/6-31G (d, p) to predict the molecular structure and vibrational wave numbers [xxi]. Calculations were carried out with Beck's three parameter hybrid model using the Lee-Yang-Parr correlation functional (B3LYP) method. The structure optimization was performed to identify the optimized structure and geometry of the examined species. The unscaled wave number was scaled down using the scale factor value of 0.920 for DFT method. The DFT hybrid B3LYP functional methods have to be used for obtaining a considerably better agreement with experimental data [xxii-xxv].

3. Result and Discussion

3.1. Structural determination by ^{1}H NMR and ^{13}C NMR spectra

→ 6-(2-phenylhydrazono)-tetrahydro-2-thioxopyrimidin-4(1H)-one

The ^{1}H NMR spectrum of PHTTO were recorded in DMSO-d^{6}solvent. There is a singlet at δ 1.163 ppm integrated to 2H which should be the CH_2 methylene proton. The NH protons exhibited two characteristic broad singlets at δ 9.946 ppm and 10.922 ppm of NH present in thiobarbituric acid. The NH attached to phenyl ring is observed at δ 5 ppm. The signals of aromatic CH protons are observed as a multiplet at δ 8.75, 8.17-8.20, 7.60-7.62 respectively.

The *^{13}C NMR* spectra of PHTTO (DMSO-d^{6}) are assigned as follows where the phenyl ring shows signals at δ 123.45, 127.48, 129.53, 115.55 ppm. The C=N hydrazone linkage is observed at δ 149.14 ppm, where the C-N Phenyl linkage is assigned at δ 134.20 ppm. The CH_2 carbon of methylene proton is assigned at δ 44.21 ppm, the C=O and C=S functional group are observed at 155.74 ppm and 163.45 ppm. The spectra are shown below in Fig 3 and Fig 4.

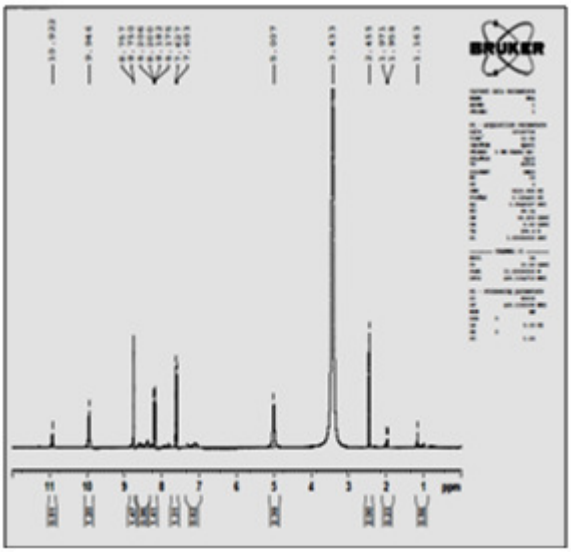

Figure 3

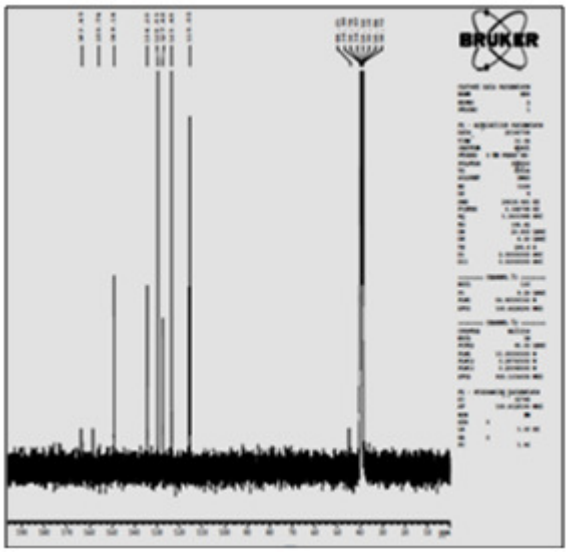

Figure 4

4. Molecular Geometry

The optimized molecular structure of the title compound shown below is determined by using B3LYP/6-31G (d, p) level of calculation.

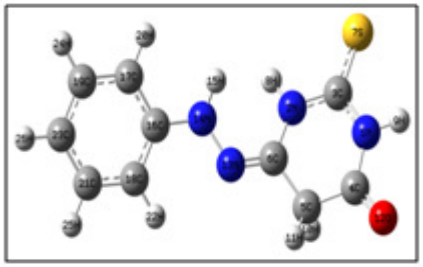

Figure 5

From the bond parameters most of the optimized bond lengths are slightly longer than the experimental values, the bond angles and dihedral angles are slightly different from the experimental angles. We note that the experimental results are calculated at solid phase and the theoretical calculations are calculated at gas phase. In the solid state, the existence of a crystal field along with the intermolecular interactions connect the molecules together, which results in the differences in bond parameters between the calculated and experimental values. The C-S and C-O bond length is 1.6627 Å, 1.2123 Å respectievely which is typical for a C=S double bond (sp2 hybridized) [xxvi] and carbonyl group [xxvii].Bond distances in hetero aromatic rings changed due to difference in electronegativity of the atom present. In hydrazone group, C6-N13double bond distance is about 1.2831 Å is found related to hydrazone structures, i.e. 1.2810 Å and 1.272 Å [xxviii]. The Thiopyrimidone ring and phenyl ring exhibits an approximately perpendicular conformation i.e. C6-N13-N14 (116.74°) is inclined at 90°with N13-N14-C16 (117.85°) due to bond strains. The bond lengths and angles in the pyrimidone ring are similar to 2-thiobarbituric acid [xxix] and isopropylidine thiobarbituric acid [xxx].The molecular structure demonstrated that the imination occurred on oxygen atom of thiobarbituric ring and the Nitrogen atom which is far from phenyl ring. The longerC10–C11 bond distance (1.48Å) shows that there is no delocalization of the nitrogen lone pair of electrons towards the ring. This indicates the delocalization of electrons in the central part of the molecule [xxxi].The experimental N-N bond length of title compound is reported as 1.3738 Å which coincides with the electron diffraction N-N bond length of tetra-methyl hydrazone is reported at 1.401Å [xxxii-xxxiii].The C-H bond distance of active methylene group is 1.08 Å (C5-H11), 1.10 Å (C5-H10) which is more or less equal with phenyl skeletal ring. The calculated bond lengths of the C–C bond in benzene ring is between 1.392 Å - 1.501Å, while experimentally, it ranges 1.365–1.500Å which is much shorter than the typical C–C single bond (1.54 ˚A) and longer than the C=C double bond (1.34Å)[xxxiv-xxxv].

The torsional angles of C16–N14–N13–C6, C5–C6–N13–N14, C17-C16-N14-N13, C18-C16-N14-N13, N2–6C–N13–N14 are -179.24, -2.06, 179.76, 161.17, -21.47 respectively, show that the molecule itself is not planar. Where C16 and C6, C5 and N14, C17 and N13 are trans to each other whereas N2, N14and C18, N13 are cis to each other.

5. Vibrational Assignments

The PHTTO molecule consists of 26 atoms and so it has 72 normal vibrational modes. The vibrational band assignments have been made based on SQM program. The theoretical DFT force field was transformed from Cartesian coordinates into the local coordinates and then scaled empirically according to the SQM procedure [xxxvi].

$$F_{ij}^{scaled} = (CiCj)^{1/2} F_{IJ}^{B3LYP} \text{--------(1)}$$

Ci- scale factor of coordinate i,

F_{IJ}^{B3LYP}- B3LYP/6-31Gforce constant in local coordinate, and

F_{ij}^{scaled} - scaled force constant.

The assigned frequencies as predicted from the basis set B3LYP/ 6-31G (d, p) is nearly same expect for slight variations in the potential energy distributions. The observed and simulated FT-IR and Raman spectra of PHTTO are given in Figs. 6&7 respectievely. The calculated spectra are found to be close to the experimental values reveals the overestimation of the calculated vibrational modes due to neglect of an-harmonicity in real system [xxxvii] as shown in Table1.

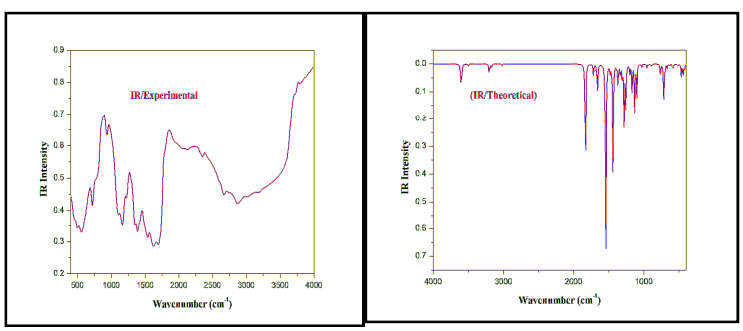

Figure 6: the recorded and theoretical FT-IR spectra of PHTTO

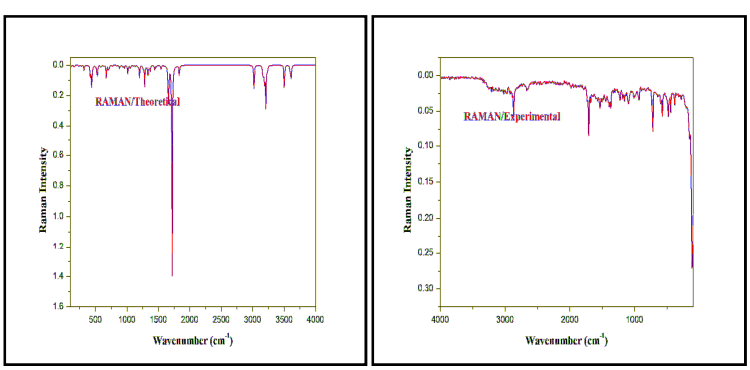

Figure 7: the recorded and theoretical FT-Raman spectra of PHTTO

Mode No.	Un-scaled Freq	Scaled freq	IR	Raman	Intensity		TED≥10%
					IR	Raman	
1	3503	3365	3186 w	3107 w	1.80	1.88642	$\nu N_{14}H_{15}(99)$
2	3168	3043	3014 w	3022 m	2.49	0.52935	$\nu C_{17}H_{20}(90)$
3	3164	3039	2870 m	2924 w	0.005	0.99309	$\nu C_5H_{11}(97)$
4	3023	2904	2667 m	2869 s	1.82	3.5551	$\nu C_5H_{10}(96)$
5	1833	1761	1697 w	1709 s	81.42	4.73621	$\nu C_4O_{12}(86)$
6	1718	1650	1625 m	1680 m	8.64	100	$\nu C_6N_{13}(84)$
7	1663	1597	-	1571 w	23.57	20.1724	$\nu C_{17}C_{19}(60)+\beta C_{17}C_{16}C_{18}(25)$
8	1651	1586	1537 w	1535 s	1.52	4.03796	$\nu C_{21}C_{23}(25)+\nu C_{16}C_{18}(35)+\beta C_{23}C_{19}C_{17}(15)$
9	1553	1491	-	1503 w	29.00	0.50552	$\beta H_9N_1C_3(12)+\beta H_8N_2C_3(18)+\beta H_{15}N_{14}C_{16}(15)$
10	1479	1420	-	1444 w	5.82	0.26835	$\nu C_{18}C_{21}(12)+\beta H_{15}N_{14}C_{16}(22)+\beta H_{24}C_{19}C_{23}(15)+\beta H_{26}C_{23}C_{21}(15)$
11	1439	1382	1386 w	1391 s	78.04	2.66941	$\nu C_3N_2(35)+\nu C_2N_1(30)+\beta H_9N_1C_3(12)$
12	1389	1334	-	1368 s	2.10	0.05532	$\beta H_9N_1C_3(28)+\beta H_8N_2C_3(38)$
13	1370	1316	-	1327 w	9.23	2.50522	$\nu C_{16}C_{18}(32)+\nu C_6N_3(20)$
14	1281	1230	1222 w	1223 s	40.65	13.952	$\nu C_{16}N_{14}(35)$
15	1202	1154	-	1182 m	1.01	4.4196	$\beta H_{20}C_{17}C_{19}(25)+\beta H_{22}C_{18}C_{21}(18)+\beta H_{24}C_{19}C_{23}(20)$
16	1167	1121	1163 m	1156 m	24.15	1.57658	$\nu C_3N_1(15)+\nu N_{14}N_{13}(18)+\nu C_5S_7(22)+\beta H_9N_1C_3(12)$
17	1131	1086	1105 w	1093 s	32.26	1.10784	$\nu N_{14}N_{13}(25)$
18	963	925	933 w	931 m	0.035	0.05679	$\tau H_{20}C_{17}C_{19}H_{24}(52)+\tau H_{22}C_{18}C_{21}H_{25}(25)$
19	767	736	723 m	722 s	9.368	2.05061	$\Gamma C_{17}C_{16}C_{19}H_{20}(18)+\tau H_{26}C_{23}C_{21}C_{18}(32)+\Gamma N_{14}C_{16}C_{18}C_{17}(20)$
20	579	556	559 w	574 s	1.368	2.06385	$\Gamma O_{12}C_5N_1C_4(30)$
21	504	484	497 w	482 s	0.59	1.94527	$\beta C_5C_4N_1(35)$
22	469	450	-	445 s	8.68	1.66132	$\beta C_5C_4O_{12}(30)+\beta C_{18}C_{16}N_{14}(12)+\beta C_4C_5C_6(15)$
23	443	425	-	385 s	9.80	84.1518	$\Gamma N_{14}C_{16}N_{13}H_{15}(35)$
24	319	306	-	283 w	1.19	23.064	$\tau C_5C_6N_{13}N_{14}(32)$
25	164	157	-	154 w	1.86	23.4586	$\beta N_2C_3S_7(12)+\tau C_5C_3C_6N_2(15)$
26	118	113	-	114 s	0.71	16.9525	$\beta C_{16}N_{14}N_{13}(12)+\tau N_1C_4C_3N_2(65)$

Table 1: Vibrational Assignments of PHTTO by B3LYP/6-31G (d, p) method

The CH stretching vibrations give rise to bands in the region 3100–3000 cm^{-1} in aromatic compounds. Where C-H stretching vibrations are not mixed with other type of vibrations. The CH in-plane bending vibrations are observed in the region 1300–850 cm^{-1} and are usually of medium to weak intensity. The CH out-of-plane bending modes are usually of weak intensity and are observed in the region 950–600 cm^{-1}[xxxviii-xl]. From PED analysis the stretching frequency of CH aromatic is observed in experimental spectrum at 3014 cm^{-1} in IR spectra and at 3022 cm^{-1} in FT-Raman spectra. The CH in plane and out of plane bending vibrations are occur near the region 933 cm^{-1} and 723 cm^{-1} in IR spectrum, further the FT-Raman spectrum near 931 cm^{-1} and 722 cm^{-1} respectievely with PED% of about 90%, 52%, 32%.The carbon – carbon stretching modes of the phenyl ring are expected to be in the range from 1650 -1200 cm^{-1}[xli-xlii]. In the Raman spectrum of title compound, the carbon–carbon stretching bands appeared at 1535, 1503, 1327, 1011 cm^{-1} its PED contribution is ~ 30 % and in IR spectrum at 1537 cm^{-1}. The theoretically calculated values by B3LYP method are 1650, 1597, 1316 and 1011 $cm^{-1}$and these values show excellent agreement with above experimental data. The C=O stretching vibrations are normally observed in the range of 1800–1600 cm^{-1}[xliii]. On the other hand, this mode gives only weak or very weak absorptions in Raman spectroscopy. In our study, as expected, C=O functional group of title compound is observed at 1697 cm^{-1} in IR spectrum and 1709 cm^{-1} in Raman spectrum, which is in excellent agreement with the calculated value of 1761 cm^{-1}. *Rumyana et al*[xliv] assigned C=O of thiobarbituric at 1722 cm^{-1} which coincides with our experimental value of PHTTO.NH groups are very characteristic and their stretching vibrations are observed, in many cases, around 3500– 3300 cm^{-1} [xlv-xlvi]. For PHTTO the NH vibration was observed as a weak band located at 3186 cm^{-1} in IR spectrum and 3107 cm^{-1} in Raman spectrum and it is theoretically observed at 3365 cm^{-1} at mode no. 3 and PED assignment of about 99%. *Mendez et al* [xxviii] and *Ramando et al* [xlvii] observed NH stretching frequency at 3587 cm^{-1}, 3430 cm^{-1}.The N-N stretching frequency was assigned to the medium intensity in IR and Raman bands at 1105 cm^{-1} and 1093 cm^{-1} which coincides very well with scaled wavenumbers at 1086 cm^{-1}. (PED value of about 25%).The methylene group has six vibrational modes asymmetrical, symmetrical stretching, scissoring, wagging, twisting and rocking modes. The CH_2 asymmetric stretching is usually observed at 3000 cm^{-1}, the CH_2 symmetric stretching frequency is assigned between 3000-2900 cm^{-1}[xlvii-xlviii]. For the title compound, the CH_2 stretching modes (asymmetric and symmetric modes) are observed at 2870 cm^{-1} in IR spectrum and 2667 cm^{-1} in Raman spectrum respectively and the symmetric mode is detected at 2667 cm^{-1} in IR and 2869 cm^{-1} in Raman spectrum and they well coincide with the scaled wave numbers 3039 cm^{-1} and 2904 cm^{-1} (TED = 97%, 96**%)** respectievely. The C=S group is less polar than the C=O group and has a considerably weak band. Compound that contains a thiocarbonyl groups shows absoprtion in the region 1250-1020 cm^{-1}[xli, xlv]. In our present study, the C=S stretching frequency is observed in the region 1163 cm^{-1} and 1156 cm^{-1} in IR and Raman spectra. The above experimental values are well coincided with the scaled theoretical value 1121 cm^{-1} obtained by B3LYP method with PED value of about 22%.The C=N stretching band are observed in the range 1627– 1566 cm^{-1}[xlix–lxi]. For the title compound the band calculated at 1650 cm^{-1} by B3LYP method is assigned to C=N stretching mode and experimentally observed in IR spectrum at 1625 cm^{-1} whereas at 1680 cm^{-1} in FT-Raman spectrum. *Hahebalzamani* et al [lxii], Lin *Vin et al* [lxiii] supported the C=N stretching frequency at 1591 cm^{-1}, 1622cm^{-1} respectievely. *Silverstein et al* assigned C-N stretching absorption in the region 1342-1266 cm^{-1} [xli]. In our title compound the C-N

vibrations are assigned at 1386 cm^{-1} in IR and at 1391 cm^{-1} in Raman respectively. Based on the results of the previous works on phenyl hydrazine derivatives the bands of the IR spectra 462-491cm^{-1} are assigned to C-N bending vibration modes. The bands in the region of 497 and 482 cm^{-1} has been assigned to symmetric C-N bending.
In order to investigate the performance and vibrational wavenumbers of the title compound root mean square value (RMS) and correlation coefficient between calculated and observed wave numbers were calculated and correlation graph is represented in Fig. 8

$$\mathbf{RMS}=\sqrt{\frac{1}{n-1}\sum(\nu_i^{cal}-\nu_i^{exp})} \text{ ------ (2)}$$

RMS values of wave numbers were evaluated using the following expression [lxiv]. The RMS error of the observed IR and Raman bands are found to be 47.67, 11.89 for DFT method. The small differences are observed since experimental vibrational modes are calculated in solid phase and Scaled vibrational modes are calculated in gaseous phase.

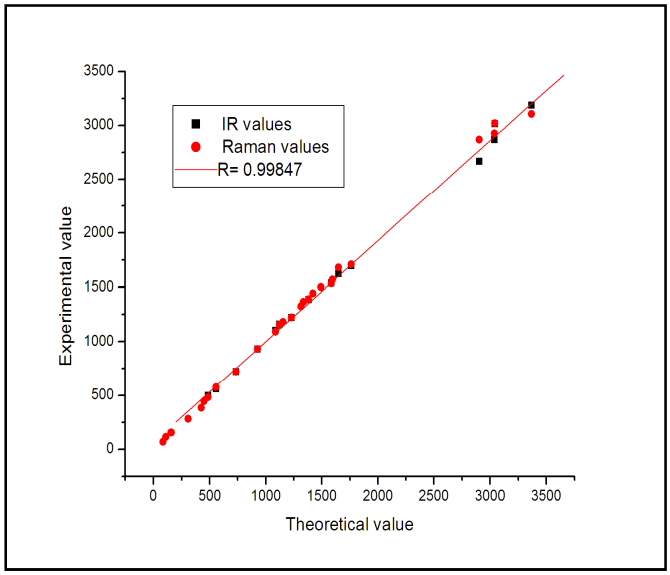

Figure 8: Correlation graph of PHTTO between experimental and theoretical values

5.1. Non-linear Optical Properties

The significance of the polarizability and the first hyperpolarizability of molecular systems depend on the efficiency of electronic communication between acceptor and the donor groups, since it is the base to intramolecular charge transfer [lxv]. The charge transfers through single-double bond conjugated path induce large variations in dipole moment and molecular polarizability whereas it is strong at IR and Raman activity. The molecular hyperpolarizability get enhanced in organic molecules containing O-H, N-H and C=O which involved in hydrogen bond interactions. From the 6-31G (d, p) basis set calculation the dipole moment (μ) was calculated at **0.8804**Debyeand α, β were calculated at 4**.0215x*10*$^{-30}$*esu***and 14.0383 **x*10*$^{-30}$*esu***respectively which is **37** times higher than the standard β_0 value of urea Table 2.

Parameters	B3LYP/6-31G(d,p)	*Hyperpolarizability (β_0) x10^{-30}esu*	
Dipole moment (μ) Debye			
μ_x	-0.8666		
μ_y	-0.0533	β_{xxx}	1815.40
μ_z	-0.1461	β_{xxy}	-36.58
μ	0.8804Debye	β_{xyy}	-224.85
		β_{yyy}	-226.57
Polarizability (α_0) x10^{-30}esu		β_{xxz}	37.03
		β_{xyz}	52.91
α_{xx}	266.54	β_{yyz}	-6.55
α_{xy}	15.61	β_{xzz}	14.43
α_{yy}	175.25	β_{yzz}	9.28
α_{xz}	-2.70	β_{zzz}	-30.24
α_{yz}	9.34	β_0	14.0383 x10^{-30}esu
α_{zz}	71.11		
α	4,0215x10^{-30}esu		

Table 2: The Non-linear optical properties of PHTTO

5.2. Frontier Molecular Orbital

On the basis of fully optimized ground state structure, B3LYPlevels with the 6-31G (d, p) basis set calculations are used to determine the low-lying excited states of 6-(2- phenylhydrazono) tetrahydro –2–thioxopyrimidin-4(1h)-one. The energy gap between the highest occupied molecular orbital (HOMO) and lowest unoccupied molecular orbital (LUMO) determines the chemical stability, optical polarizability and chemical hardness [lxvi]. The HOMO represents the ability to donate an electron, LUMO as an electron acceptor represents the ability to obtain an electron. The HOMO and LUMO energy calculated by B3LYP levels with the 6-31G (d, p) basis set are shown in Fig 9. The HOMO is located over the thiocarbonyl group; the HOMO → LUMO transition implies an electron density transfer to phenyl ring from thiobarbituric ring. The energy gap between the HOMO and LUMO is found to be 3.6761 eV and the second transition HOMO-1 → LUMO+1 is 6.1466 eV. The density of state spectrum of PHTTO was drawn by convolution the molecular orbital information with Gaussian curve of union height is shown in Fig 10. The most important application of DOS plot is to demonstrate molecular orbital composition and contribution to chemical bonding.

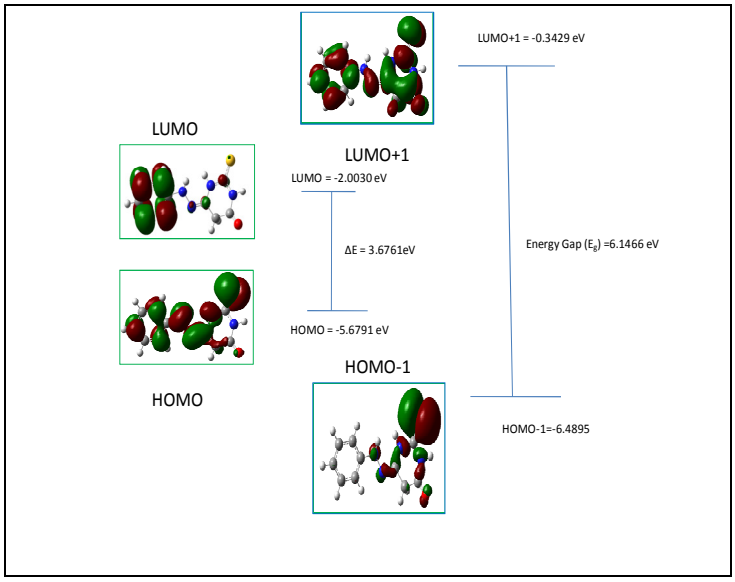

Figure 9: HOMO –LUMO diagram of PHTTO by B3LYP/6-31G (d, p) method

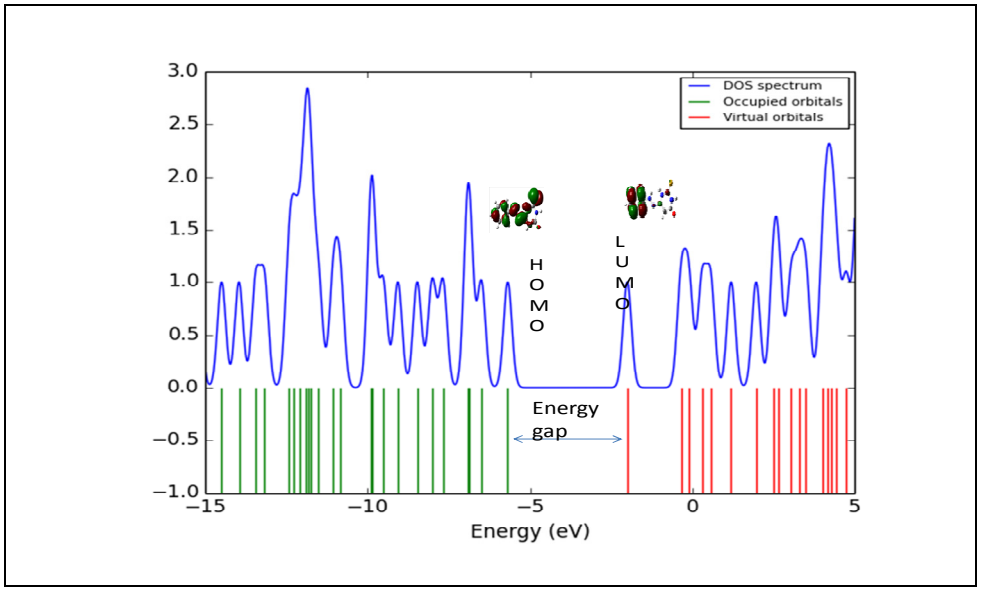

Figure 10: The density of state (DOS) Spectrum of PHTTO by B3LYP/6-31 G (d, p)

5.3. UV Spectral Analysis

The UV-Vis spectrum provides evidence confirming their molecular structures. All the structures allow strong σ → σ* or π → π* transitions in the UV-Vis region with high extinction coefficients. The λ_{max} for lower lying singlet states of the molecule have been calculated by DFT/ B3LYP/ 6-31G (d, p) method. The λ_{max}, oscillator strength and excitation energies of PHTTO are reported. UV Visible absorption corresponds to the electronic transition between frontier orbitals of PHTTO. The observed UV-Vis Spectrum was shown in Fig.11. As can be seen from the Fig.11, the experimental electronic absorption spectra of the title compound shows three bands at 345 nm (log ε = 0.1915), 302 nm (log ε = 0.0037), 238nm (log ε = 0.0059). The theoretical absorption bands are predicted at 386, 368,

279 nm. By comparing the experimental and calculated value the difference of 41.32 nm and 41.2 nm is obtained which shows hypsochromic shift or blue shift of λ_{max} C=N favouring n-π* and λ_{max} of phenyl favouring π-π* due to delocalization of πelectrons. Increase in polarity of the solvent generally shifts the n-π* and n-σ* bands to shorter wavelength and π-π* bands to longer wavelengths. In TD-DFT method the electronic absorption spectra for different solvents and gas phase are shown in Fig.12. By comparing the experimental and theoretical method π-π* transition is favoured.

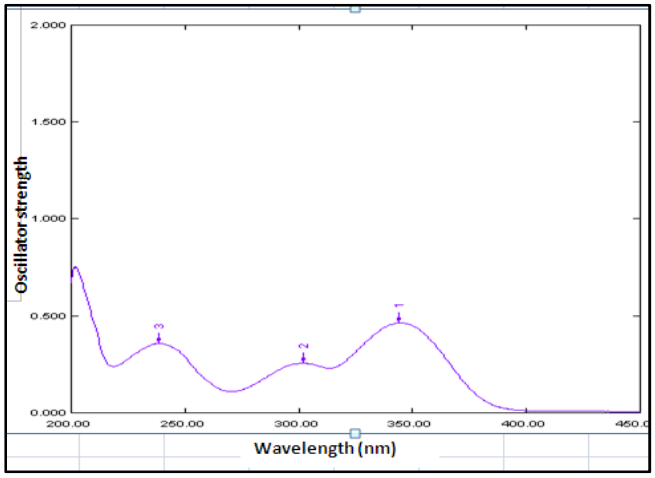

Figure 11: Experimental and calculated electronic spectra of the studied compounds using TD-DFT Method

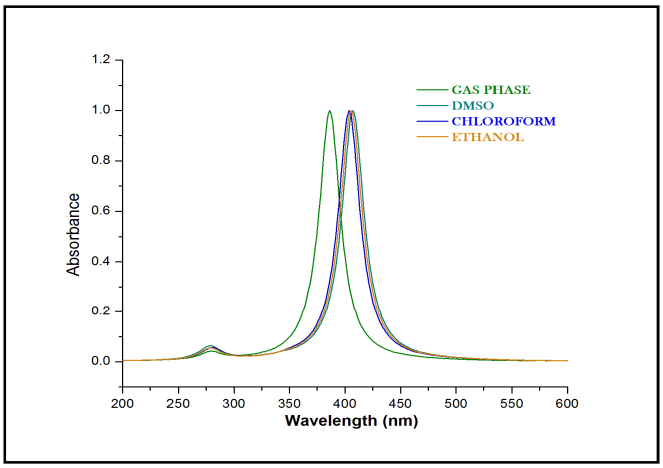

Figure 12: Theoretical Electronic Absorption spectra of different solvents by B3LYP/6-31G (d, p)

5.4. NBO Analysis

NBO analysis provides information about intra and intermolecular bonding, interaction between both filled and virtual orbitals, charge transfer and conjugative interactions in molecular system. The conjugation gives stabilization to the molecule by overlap between an occupied orbital with neighboring electron deficient orbital.

Natural bond orbital (NBO) analysis allows the assignment of the hybridisation of atomic lone pairs and the atoms involved in bond orbitals. Interaction between atomic orbitals (filled donors) – Lewis type NBO'S and empty (acceptors) non-Lewis NBO's are reported. Some electron donor orbital, acceptor orbital and the interacting stabilization energy results in second order microdisturbance theory is reported [lxvii]. In addition, the occupancy of natural bonds and lone pairs, and the percentage of p character calculated by NBO analysis method are given. The stabilization energy $\Delta E_{i,j}$ associated with delocalization is estimated by the second order perturbative as

$$\mathbf{E^{(2)} = \Delta E\ i, j = q_i \frac{F(i,j)^2}{\varepsilon_j - \varepsilon_i}} \text{--------(3)}$$

q_i – donor orbital occupancy

εi, εj – diagonal elements (orbital energies)

F (i, j) – off diagonal NBO Fock or Kohn – Sham matrix element. [lxviii]

E (2) – Stabilization Energy.

From Table3 the most important interaction n (LP (1) N_1)→π*(C_3-S_7), n(LP (1) N_2→π*(C_3-S_7), n(LP(1)N_1→π*(C_4-O_{12}), n(LP(1)N_2→(C_6-N_{13}), n(LP(2)O_{12}→**σ***(N_1-C_4), n(LP(1)N_{14}→ π*(C_{16}-C_{18}) shows 274.55, 289.41, 202.46, 140.92, 122.84 and 103.89 KJ/mol shows higher stabilization energy for carbonyl and thiocarbonyl moieties of thiobarbituric ring. The transition of phenyl ring occurs

between C_{16}-C_{18} →C_{17}-C_{19}→C_{21}-C_{23} have stabilization energy of about 76.07, 93.14, 90.17 and 77.45 respectievely. From the intra-molecular hyperconjugative interactions are formed by the orbital overlap between π(c-c)→ π*(c-c) bond orbitals which results in stabilization of the ring system. These interactions weaken the respective bonds. The ED at the six conjugated π bonds ($\sim 1.64, 1.70, 1.66\ e$) to π*(∼0.34, 0.39, 0.39 e) of the phenyl ring clearly demonstrates strong delocalization leading to stabilization of phenyl ring. The π electron cloud movement from donor to acceptor can make the molecule high polarized and must be responsible for NLO properties of PHTTO. From NBO discussion the energy transfers from thiobarbituric ring to phenyl ring have been identified.

Type	Donor(i)	ED/e	Acceptor(j)	ED/e	E(2) KJ/mol	E(j)-E(i) a.u	F(i,j) a.u
π-π*	C 3 - S 7	1.97429	C 3 - S 7	0.43914	18.54	0.22	0.031
π-π*	C16 - C18	1.64124	C17 - C19	0.34699	76.07	0.28	0.064
			C21 - C23	0.34684	93.14	0.29	0.072
π-π*	C17 - C19	1.70133	C16 - C18	0.39505	90.17	0.28	0.071
			C21 - C23	0.34684	71.34	0.29	0.063
π-π*	C21 - C23	1.66745	C16 - C18	0.39505	77.45	0.27	0.065
			C17 - C19	0.34699	95.95	0.28	0.071
n-π*	LP(1)N 1	1.63419	C 3 - S 7	0.43914	274.55	0.21	0.106
			C 4 - O12	0.21682	202.46	0.29	0.109
n-π*	LP(1)N 2	1.65197	C 3 - S 7	0.43914	289.41	0.21	0.111
			C5 - C6	0.02827	6.52	0.68	0.033
			C6 - N13	0.01621	6.11	0.89	0.035
			C6 - N13	0.262	140.92	0.29	0.091
n-π*	LP(1)N 14	1.76735	C 6 - N13	0.262	90.71	0.3	0.073

Table 3: Second order perturbation theory analysis of Fock matrix in NBO basis for PHTTO.

5.5. Electrostatic Potential Surface

MEP and electrostatic potential explains about the charge distributions in a molecule. The charge distribution explains about molecular interaction within the molecule. The reactivity of our title compound is Fig.13 in a three dimensional MEP surface. The total electron density and MEP surface of the molecule under investigation is constructed by using B3LYP/6-31G (d, p) method. MEP helps in predicting the sites for nucleophilic and electrophilic attack in the molecule by color grading, molecular size, shape and further it is useful in research for explaining the physiochemical properties of the molecule [lxix]. The region of negative charge is pictured out by red color, which indicates the electrophilic attack sites of our molecule. The red region is localized over C19, C21, C23 of phenyl ring in our title molecule. The region of positive charge is pictured out by blue color, which indicates the nucleophilic attack sites were localized over two N–H group of the thiobarbituric ring. The green color corresponds to a potential half way between the two extremes red and blue region and represents the neutral charge for nitrogen atom N13 and N14.

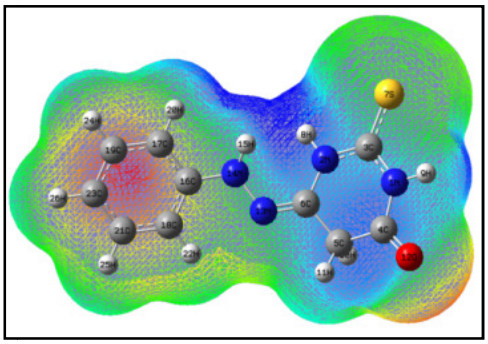

Figure 13: Molecular Electrostatic Potential diagram of PHTTO.

6. Conclusion

The geometrical parameters of the optimized structure were studied in detail and the vibrational frequency analysis by B3LYP method agrees satisfactorily with experimental results. The value of HOMO-LUMO energy gap explains chemical reactivity of the title molecule. NBO study reveals that the lone pair orbital participates in electron donation to stabilize the compound. Thus the present investigation provides complete vibrational assignments, structural information properties of the compound. The UV data indicated that the electronic transition in the compound has n- π* and π-π* transitions. The values of dipole moment (μtot), polarizability (αtot) and first-order

hyperpolarizability (βtot) of the molecule were calculated. It has been found that the value of first-order hyperpolarizability is 14.0383 × 10^{-30} *esu* which is 37 times greater than that of urea, which shows that the molecule is a good NLO material.

7. References

i. Vijay Dabholkar, Dilip Ravi, (2010).Synthesis of biginelli products of thiobarbituric acids and their antimicrobial activity, Journal of the Serbian Chemical Society. 75, 1033 - 1040. http://dx.doi.org/10.2298/jsc090106060d
ii. Mazaahir Kidwai, Ruby Thakur, Richa Mohan,(2005).A New Route to 2, 4, 6-Trisubstituted-6H-1, 3-oxazines, Chem Inform. 36, 15. http://dx.doi.org/10.1002/chin.200515150
iii. Yoshinori Kadoma, Seiichiro Fujisawa, (2012).Radical-Scavenging Activity of Thiols, Thiobarbituric Acid Derivatives and Phenolic Antioxidants Determined Using the Induction Period Method for Radical Polymerization of Methyl Methacrylate, Polymers. 4, 1025 – 1036. http://dx.doi.org/10.3390/polym4021025
iv. Khanna, Palit, Srivastava, Shanker,(1990). Chem Inform Abstract: Newer Heterocycles of Phenothiazine and Their Antiparkinsonian Activity, Chem Inform.21, 38. http://dx.doi.org/10.1002/chin.199038249
v. Mohammed Saleh, Makki, Reda Abdel-Rahman, Hassan Faidallah, Khalid Khan, (2013). Synthesis of New Fluorine Substituted Heterocyclic Nitrogen Systems Derived from p-Amino-salicylic Acid as Anti-mycobacterial Agents. Journal of Chemistry. 2013, 1-8. http://dx.doi.org/10.1155/2013/819462
vi. Archana, Srivastava, Ashok Kumar, (2004). Synthesis of some newer derivatives of substituted quinazolinonyl-2-oxo / thiobarbituric acid as potent anticonvulsant agents, Bioorganic&MedicinalChemistry. 12, 1257 -1264. http://dx.doi.org/10.1016/j.bmc.2003.08.035
vii. Louis Goodman; M.D., Alfred Gilman, (1942).The Pharmacological Basis of Therapeutics: A textbook of pharmacology, toxicology and therapeutics for physicians and medical students, New York: The Macmillan Company, Journal of Medicine. 226, 250 – 250. http://dx.doi.org/10.1056/nejm194202052260618
viii. Mushin, (1956) Thiobarbiturates, Brazilian. Med. Journal. 1, 1532 - 1532 http://dx.doi.org/10.1136/bmj.1.4982.1532-a
ix. Semenov, Levina, Krasnov,(2005). Synthesis of Indole-Containing 2-Thiobarbituric Acid Derivatives, Pharmaceutical Chemistry Journal. 39, 29 – 33. http://dx.doi.org/10.1007/s11094-005-0073-4
x. Sabir Syed Salman, Rocha, (2002) Antioxidant properties of β seleno amines against lipid per – oxidation in rat brain and liver Environmental Toxicology and Pharmacology. 34, 446 -453. http://dx.doi.org/10.1016/j.etap.2012.06.002
xi. Liang Ma Shilin Li, Hao Zheng, Jin ying Chen, Lin Lin, Xia Ye, Zhizhi Chen, Qinyuan Xu, Tao Chen, Jincheng Yang, Neng Qiu, Guangcheng Wang, Aihua Peng, Yi Ding, Yuquan Wei, Lijuan Chen,(2011).Synthesis and biological activity of novel barbituric and thiobarbituric acid derivatives against non-alcoholic fatty liver disease, European Journal of Medicinal Chemistry. 46, 2003-2010. http://dx.doi.org/10.1016/j.ejmech.2011.02.033
xii. Mohamed, Yassin, Khalil, Sabaa, (2000). Organic thermal stabilizers for rigid poly(vinyl chloride) I. Barbituric and thiobarbituric acids in Polymer Degradation and Stability.70, 5 -10.http://dx.doi.org/10.1016/s0141-3910(00)00054-9
xiii. Dongli Zhang, Junbo Zhang, Mengjie Li, Wenli Li, Gulibahaer Aimaiti, Gulibosidan Tuersun, Jiannong Ye, Qingcui Chu, (2011). A novel miniaturized electrophoretic method for determining formaldehyde and acetaldehyde in food using 2-thiobarbituric acid derivatisation,Food Chemistry.129, 206 –212. http://dx.doi.org/10.1016/j.foodchem.2011.04.025
xiv. Balas, Verginadis, Geromichalos, Kourkoumelis, Male, Hursthouse, Repana, Yiannaki Charalabopoulos, Bakas, Hadjikakou, (2011) Synthesis, structural characterization and biological studies of thetriphenyltin (IV) complex with 2-thiobarbituric acid, European Journal of Medicinal Chemistry. 46, 2835 -2844. http://dx.doi.org/10.1016/j.ejmech.2011.04.005
xv. Nagy Khalifa, Adel Abdel-Rahman, Sherein Abd-Elmoez, Omar Fathalla, Amina Abd El-Gwaad, (2013). A convenient synthesis of some new fused pyridine and pyrimidine derivatives of antimicrobial profiles, Research on Chemical Intermediates. 41, 2295 – 2305. http://dx.doi.org/10.1007/s11164-013-1347-1
xvi. Jacek Bojarski, Jerzy Mokrosz, Henryk Barton, Maria Paluchowska, (1985). Recent Progress in Barbituric Acid Chemistry, Advances in Heterocyclic Chemistry. 229 -297. http://dx.doi.org/10.1016/s0065- 2725(08)60921-6
xvii. Osman, Kandeel, Said, Ahmed, (2010).Synthesis and Anticonvulsant Activity of Some Spiro Compounds Derived from Barbituric and Thiobarbituric Acids, Chem Inform Abstract. 27, 52. http://dx.doi.org/10.1002/chin.199652179
xviii. Zalukaev, Trostyanetskaya, (1971). Reaction of barbituric acid with α, β - unsaturated ketones, Chemistry of Heterocyclic compounds. 7, 781 - 782. http://dx.doi.org/10.1007/bf00476833
xix. Joost Cornelissen, John Van Diemen, Lucas Groeneveld, Jaap Haasnoot, Anthony Spek Jan Reedijk, (1992). Synthesis and properties of isostructural transition-metal (copper, nickel, cobalt, and iron) compounds with 7,7',8,8'-tetracyanoquinodimethanide(1-) in an unusual monodentate coordination mode: crystal structure of bis(3,5-bis(pyridin-2-yl)-4-amino-1,2,4-triazole)bis(7,7',8,8'tetracyanoquinodimethanido)copper(II),Inorganic Chemistry. 31, 198-202. http://dx.doi.org/10.1021/ic00028a014
xx. Dalip Kumar, Maruthi Kumar, Soumitra Ghosh, Kavita Shah, (2012). Novel bis (indolyl) hydrazide–hydrazones as potent cytotoxic agents, Bioorganic & Medicinal Chemistry Letters. 22,212 215. http://dx.doi.org/10.1016/j.bmcl.2011.11.031

xxi. Effenberger, Breyer, Schobert,(2010). Modulation of doxo rubicin activity in cancer cells by conjugation with fatty acyl and terpenyl hydrazones, European Journal of Medicinal Chemistry. 45, 1947 -1954. http://dx.doi.org/10.1016/j.ejmech.2010.01.037

xxii. Srinivasan Iyengar, Bernhard Schlegel, John Millam, Gregory Voth, Gustavo Scuseria, Michael Frisch,(2001). Ab initio molecular dynamics: Propagating the density matrix with Gaussian orbitals. II. Generalizations based on mass-weighting, idem potency, energy conservation and choice of initial conditions, The Journal of Chemical Physics. 115, 10291-10313. http://dx.doi.org/10.1063/1.1416876

xxiii. Axel Becke, (1993). Density - functional thermochemistry. III. The role of exact exchange, The Journal of Chemical Physics.98, 5648 - 5655. http://dx.doi.org/10.1063/1.464913

xxiv. Sundius, (1990). Molvib - A flexible program for force field calculations, Journal of Molecular Structure.218,321-326.http://dx.doi.org/10.1016/0022 2860(90)80287-t

xxv. Eggers, Lingren, (1956). C-H Vibrations in Aldehydes, Analytical Chemistry. 28, 1328 – 1329. http://dx.doi.org/10.1021/ac60116a032

xxvi. William Kemp, (1991). Organic Spectroscopy. http://dx.doi.org/10.1007/978-1-349-15203-2

xxvii. Allen, (1984). The current status of crystallographic database, Acta Crystallographica Section A Foundations of Crystallography . 40, 441-442. http://dx.doi.org/10.1107/s0108767384087006

xxviii. Eduardo Mendez, María Cerda, Jorge Gancheff, Julia Torres, Carlos Kremer, Jorge Castiglioni, Martina Kieninger, Oscar Ventura, (2009).Tautomeric Forms of 2-Thiobarbituric Acid As Studied in the Solid, in Polar Solutions, and on Gold Nanoparticles. The Journal of Physical Chemistry.111, 3369 -3383. http://dx.doi.org/10.1021/jp0628176

xxix. Qi Ma, Li-Ping Lu, Miao-Li Zhu, (2008).1,2-Bis(2-furylmethylene) hydrazine, Acta Crystallographica Section E. 64, o2026o2026. http://dx.doi.org/10.1107/s1600536808030729

xxx. Nicolay Golovnev, Maxim Molokeev, Liudmila Tarasova, Victor Atuchin, Natalya Vladimirova, (2014). The 5- (iso-propylidene) – 2 - thiobarbituric acid: Preparation, crystal structure, thermal stability and IR-characterization, Journal of Molecular Structure. 1068,216-221. http://dx.doi.org/10.1016/j.molstruc.2014.04.024

xxxi. Ravikumar, Hubert Joe, Jayakumar,(2008). Charge transfer interactions and optical proper-ties of push pull chromophore benzaldehyde phenyl hydrazone: A vibrational approach Chemical Physics Letters. 460,552-558. http://dx.doi.org/10.1016/j.cplett.2008.06.047

xxxii. Kunio Kohata, Tsutomu Fukuyama, Kozo Kuchitsu, (2008). Molecular structure of hydrazine as studied by gas electron diffraction, The Journal of Physical Chemistry. 86, 602 – 606. http://dx.doi.org/10.1021/j100394a005

xxxiii. Naumov, Litvinov, Geise, Dillen, (1983). The molecular structure of tetra methyl hydrazine: A gas phase electron diffraction study, Journal of Molecular Structure. 99, 303-307. http://dx.doi.org/10.1016/0022-2860(83)90033-9

xxxiv. Quack, Stockburger; M., (1972). Resonance fluorescence of aniline vapour, Journal of Molecular Spectroscopy. 43, 87 – 116. http://dx.doi.org/10.1016/0022-2852(72)90164-6

xxxv. David Lide, (1962). A survey of carbon-carbon bond lengths, Tetrahedron. 17, 125 – 134. http://dx.doi.org/10.1016/s0040-4020(01)99012-x

xxxvi. Jon Baker, Andrzej Jarzecki, (1998). Peter Pulay Direct Scaling of Primitive Valence Force Constants: An Alternative Approach to scaled Quantum Mechanical Force Fields, The JournalofPhysicalChemistryA.102,1412-1424.http://dx.doi.org/10.1021/jp980038m

xxxvii. Long, (2004).Infrared and Raman characteristic group frequencies. Tables and charts George Socrates John Wiley and Sons, Ltd, Chichester, Third Edition, 2001. Journal of Raman Spectroscopy. 35, 905-905. http://dx.doi.org/10.1002/jrs.1238

xxxviii. Krimm, Bellamy, (1975). The infrared spectra of complex molecules, 3rd edition, Halsted Press, a division of John Wiley & Sons, Inc., New York, 433. Journal of Polymer Science: Polymer Letters. (1976), 14, 121. http://dx.doi.org/10.1002/pol.1976.130140217

xxxix. Dollish, Fateley, Bentley, (1975). Characteristic Raman Frequencies of Organic Compounds, Analytica Chimica Acta. 75, 492-493. http://dx.doi.org/10.1016/s0003-2670 (01) 85385x

xl. Varsanyi, (1969). In Vibrational Spectra of Benzene Derivatives, Theoretical Bases For Molecular Spectroscopy. 17-84. http://dx.doi.org/10.1016/b978-0-12-714950-9.50005-3

xli. Silverstein, Kenneth Wong, Francis Webster, David Kiemle, Robert Bryce, (2015). Review of Spectrometric Identification of Organic Compounds, 8th Edition Spectrometric Identific-ation of Organic Compounds, Journal of Chemical Education. 92, 1602 - 1603 http://dx.doi.org/10.1021/acs.jchemed.5b00571

xlii. Gang Wang, Jian Wang, Han Nie, Shen-Peng Tan, Wei-Qun Shi, Dong-Mei Zhao, Mao-Sheng Cheng, (2013). Experimental and theoretical investigations on the tautomerism of 1-phenyl-2-thio-barbituric acid and its methylation reaction, Journal of Molecular Structure. 372 -379. http://dx.doi.org/10.1016/j.molstruc.2012.12.017

xliii. Leonardo Viana de Freitas, Cecilia da Silva, Javier Ellena, Luiz Antônio Sodré Costa, Nicolás Rey, (2013).Structural and vibrational study of 8-hydroxyquinoline-2-carboxaldehyde iso-nicotinoyl hydrazone – A potential metal–protein attenuating

compound (MPAC) for the treatment of Alzheimer's disease Spectrochimica Acta Part A: Molecular and Biomolecular Spectroscopy. 116, 41 -48. http://dx.doi.org/10.1016/j.saa.2013.06.105

xliv. Rumyana Bakalska, Vassil Delchev, (2012). Comparative study of the relaxation mechanisms of the excited states of cytosine and iso-cytosine, Journal of Molecular Modeling. 18, 5133 – 5146. http://dx.doi.org/10.1007/s00894-012-1506-0

xlv. Chishti, Muchkund Dubey, (1997). An Unequal Treaty: World Trading Order after GATT. New Delhi; New Age International Limited Publishers, 1996, 152. South Asian. 4, 186-188. http://dx.doi.org/10.1177/097152319700400117

xlvi. Avadhesh Kumar Yadav, Gautam, (2015). Synthesis, Structural and Optical Studies of Barium, Strontium, Titanate Borosilicate Glasses Doped with Ferric Oxide, Spectroscopy Letters.48,514 -520. http://dx.doi.org/10.1080/00387010.2014.920886

xlvii. Csizmadia, (1978). Theory and practice of MO calculations on organic molecules Elsevier scientific publishing company, Amsterdam, Oxford, New York, 1976.International Journal of Quantum Chemistry. 13, 159. http://dx.doi.org/10.1002/qua.560130113

xlviii. Nicolay Golovnev, Maxim Molokeev, Liudmila Tarasova, Victor Atuchin, Natalya Vladimirova, (2014).The 5-(isopropylidene)-2-thiobarbituric acid: Preparation, crystal structure, thermal stability and IR-characterization, Journal of Molecular Structure. 1068, 216-221. http://dx.doi.org/10.1016/j.molstruc.2014.04.024

xlix. Fabio Ramondo, Andrea Pieretti, Lorenzo Gontrani, Luigi Bencivenni, (2001). Hydrogen bonding in barbituric and 2-thiobarbituric acids: a theoretical and FT-IR study, Chemical Physics.271, 293 – 308. http://dx.doi.org/10.1016/s0301-0104(01)00440-2

l. Cerda, Jorge Gancheff, Julia Torres, Carlos Kremer, Jorge Castiglioni, Martina Kieninger, Oscar Ventura, (2001). Tautomeric Forms of 2-Thiobarbituric Acid As Studied in the Solid, in Polar Solutions, and on Gold Nanoparticles, The Journal of Physical Chemistry C. 111, 3369 -3383. http://dx.doi.org/10.1021/jp0628176

li. Hajar Sahebalzamani, Farshid Salimi, Elmira Dornapour, (2013).Theoretical Studies of Structure, Spectroscopy, and Properties of a New Hydrazine Derivative. Journal of Chemistry. 2013, 1 - 6. http://dx.doi.org/10.1155/2013/187974

lii. Daimay Lin-Vien, Norman Colthup, William Fateley, Jeanette Grasselli,(1991). Alkenes Chapter published 1991 in The Handbook of Infrared and Raman Characteristic Frequencies of Organic Molecules.73, 94. http://dx.doi.org/10.1016/b978-0-08-057116-4.50012-2

liii. Ushakumari, Hema Tresa Varghese, Yohannan Panicker, Tugba Ertan, Ilkay Yildiz, (2008). Vibrational spectroscopic studies and DFT calculations of 4-fluoro- N - (2-hydroxy-4-nitrophenyl) benzamide, Journal of Raman Spectroscopy. 39, 1832 – 1839. http://dx.doi.org/10.1002/jrs.2047

liv. Eric Ainscough, Andrew Brodie, Aaron Dobbs, John Ranford, Joyce Waters, (1998). Anti -tumour copper(II) salicylaldehyde benzoyl hydrazone (H2sb) complexes: Physico -chemical properties and the single-crystal X-ray structures of [{Cu(H2sb)(CCl3CO2)2}2] and [{Cu(Hsb) (ClO4) (C2H5OH)}2] and the related salicylaldehyde acetyl hydrazone (H2sa)complex, [Cu(Hsa)Cl(H2O)]•H2O, Inorganica Chimica Acta. 267, 27-38. http://dx.doi.org/10.1016/s0020-1693(97)05548-5 A

lv. Wolinski, Hinton, pulay, (1990). Journal of American chemical society. 112, 8251-8260. http://dx.doi.org/10.1021/ja00179a005

lvi. Robert Parr, Laszlo Szentpaly, Shubin Liu, (1999). Electrophilicity Index, Journal of the American Chemical Society. 121, 1922 – 1924. http://dx.doi.org/10.1021/ja983494x

lvii. Alan Reed, Robert, Weinstock, (1985). Frank Weinhold Natural population analysis, The Journal of Chemical Physics. 83, 735-736. http://dx.doi.org/10.1063/1.449486

lviii. Parthasarathi, Padmanabhan, Elango, Subramanian, Chattaraj, (2004). Intermolecular reactivity through the generalized Electrophilicity concept, Chemical Physics Letters. 394, 225- 230. http://dx.doi.org/10.1016/j.cplett.2004.07.002

lix. Stephen Carpenter, Jonathan Cole, James Kitchell, (1998). Michael Pace Center for Limnology, University of Wisconsin, 680 N. Park St., Madison, Wisconsin 53717, Limnology and Oceanography .43, 73-80. http://dx.doi.org/10.4319/lo.1998.43.1.0073